THE IMPACT OF THICKNESS MEASUREMENT ON PREDICTING RESIDUAL STRESSES DUE TO WINDING

By

J. K. Good[1], C. Mollamahmutoglu[2], R. Markum[1], and J. W. Gale[1]
[1]Oklahoma State University, USA
[2]Yildiz Technical University, TURKEY

ABSTRACT

Axisymmetric winding models were initially developed to deal with web thickness variations that were manifested in the machine and cross machine direction. The web thickness variation is a prime input to these models. Small web thickness variations can integrate during winding to produce large residual stress variation in the wound roll. Web thickness measurement in process lines employ sensors that scan over the web width while the web is moving in the machine direction. Spatially this provides a measure of web thickness in a zig-zag pattern. This thickness variation is used as a control feedback parameter that control a forming or coating die lip to reduce the web or coated web thickness variation. The scan rate of the sensor will typically be set to capture thickness data at a frequency higher than the frequency response of the control/actuator system. Is thickness data captured spatially at this rate for the process sufficient for input to the axisymmetric winding model? This publication addresses this problem. The web thickness variation of an existing web was fully mapped in the machine and cross machine directions. This data was interrogated to determine what thickness data would have been recorded at varied scan rates. The full map of thickness data was input to the winding model as well as data that would have resulted from various rates of zig-zag scanning. Results show that as the rate of zig-zag scanning increase, that the residual winding stresses converge toward the stresses produced by the input of the full thickness map. Model results were compared to test results for validation.

INTRODUCTION

Webs are made by many manufacturing processes. Plastic films are made by casting or orientation processes. Metal webs are made by rolling or casting processes. Non-wovens are made by spinning, bonding and entanglement processes. Paper is made largely using the Fourdrinier process. Web thickness variation results at various scales for these processes. On-line mass measurement from which thickness is inferred is employed

in almost all web making processes. This is typically a spot measurement and the instrument scans laterally across the web in the Cross Machine Direction (CMD) while the web travels through the process in the Machine Direction (MD). These zigzag traces of web thickness are used in closed loop process control of the formation in an attempt to achieve uniformity in thickness.

Webs often have value added in roll-to-roll (R2R) manufacturing processes. The value may come in many forms such as a coating added over the entire web width which may provide an oxygen barrier or perhaps conductivity, amongst many possibilities, depending on the requirements of final products. These coating processes are also imperfect and can lead to coated web thickness variation. Again scanning spot thickness measurement is often employed to assess the uniformity in thickness of the coated web. If the coating thickness is found to exceed limits, based on product needs, the measurements can be employed in closed loop control of the coating process. In some cases the coatings may be intentionally non-uniform. Flexible electronics are the result of discrete coatings that have been added to webs and lead to discrete thickness variation.

Webs are often wound into rolls as this is the most convenient means of storage. A given web may be unwound and rewound several times as R2R manufacturing processes are often velocity dependent. The shape of the wound roll and the internal stresses are known to be functions of the winding stress, the orthotropic modulus properties of the web, the stiffness of the core and the start and finish radius of the roll. Axisymmetric winding models have been used to demonstrate the impact that web thickness variation can have on the wound roll. To date the published examples are for cases wherein the thickness varies in the CMD but is assumed to persist in the MD. The deformed shape and internal stresses in a wound roll are influenced by the total thickness variation in the MD and CMD.

An objective of this publication is to map the thickness of a web in the MD and CMD and then to demonstrate how little is known about web thickness variation from the traditional spot zigzag measurements used for process control. Another objective will be to demonstrate what level of thickness measurement is needed to accurately characterize the internal stresses and the deformed radius of a wound roll.

WEB THICKNESS MEASUREMENT

Many web processes employ instruments which assess web mass by transmitting beta-ray, x-ray or infrared radiation through the web[1]. A collector on the opposite side of the web measures the level of radiation that passed through the web. The difference in the transmitted and collected levels of radiation is radiation that was absorbed by the web. The level of absorption is related directly to the mass of the web and with known mass density the web thickness can be inferred. Herein the thickness of a polyethylene terephthalate (PET) web will be measured by other means.

An ultrasonic method for non-contact measurement of web thickness will be employed. The material to be measured is locally oscillated using ultrasound. The transmission and reflection of this oscillation varies, depending on the mass of the web material. The oscillation amplitude is related to the web mass at the measuring point. With known mass density the thickness can be inferred. These instruments have a quoted

[1] Thermo Scientific, ATI Adaptive Technologies and Yokogawa companies are providers of these instruments.

accuracy of 0.5%. A Mesys USM-200 thickness instrument with a spot measurement diameter of 5 mm was used in this study.

Figures 1 and 2 demonstrate the ability of the USM-200 sensor to measure thickness and repeat that measurement for a PET film nominally 50 μm in thickness. In Fig. 1 two scans of thickness were measured for the same strip of web 250 cm in length. In Fig. 2 the difference of the two scans is taken. The average of the difference was taken over the 250 cm length was found as 0.063 μm. The USM-200 was set to acquire data a 10 Hz during these tests and the web velocity was 25.4 mm/s (1 in/s).

Capacitive methods are highly effective for measuring the thickness of PET film. These devices are typically non-contact and thus the capacitance of the air gaps on both sides of the web are measured in addition to the capacitance of the web[2]. The SolveTech Precision Profiler is claimed to measure thickness with an accuracy level of 0.5% and was also used in this study. The SolveTech has a rectangular measurement window that is 3.18 mm long in the MD and 57.2 mm wide in the CMD. Several measurements are taken and averaged while 3.18 mm of web passes through the measurement window. Thus each data point output is an average of the web thickness of a section of web 6.36 mm long and 57.2 mm wide that passes through the measurement window. The web velocity through the sensor was 50.8 mm/s (2 in/s).

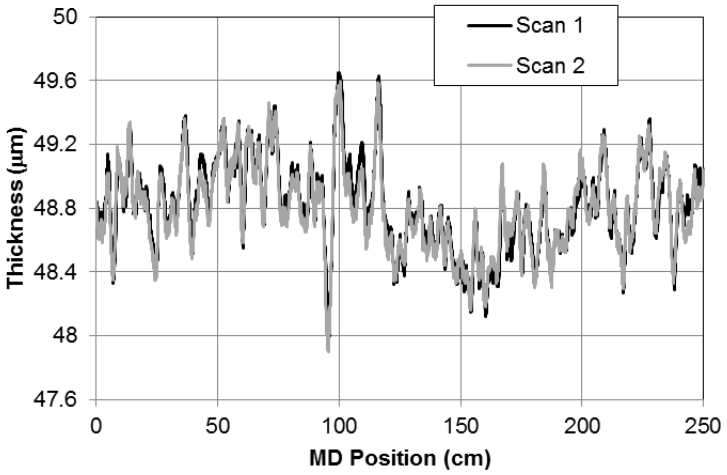

Figure 1 – Thickness of a 50 μm PET web using the USM-200.

[2] Kundig, Plast-Control, SolveTech, and TSM Control Systems companies are providers of these instruments.

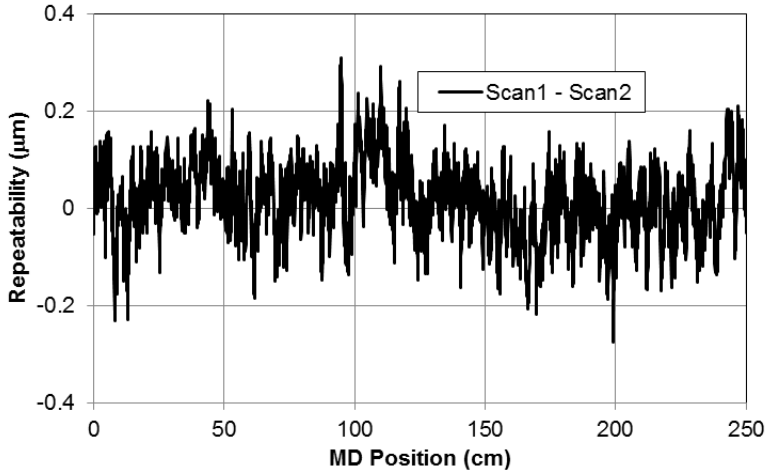

Figure 2 – Difference of Scans 1 and 2 in Fig. 1.

Figures 3 and 4 demonstrate the ability of the SolveTech Profiler sensor to measure and repeat the measurement of a PET film nominally 50 µm in thickness. In Fig. 3 two scans of thickness were measured for the same strip of web 250 cm in length, different from the strip measured in Fig. 1. In Fig. 4 the difference of the two scans is taken. The average of the difference was taken over the 250 cm length was found as 0.057 µm. Thus in these trials the repeatability of the Mesys and the SolveTech sensors were found to be very similar.

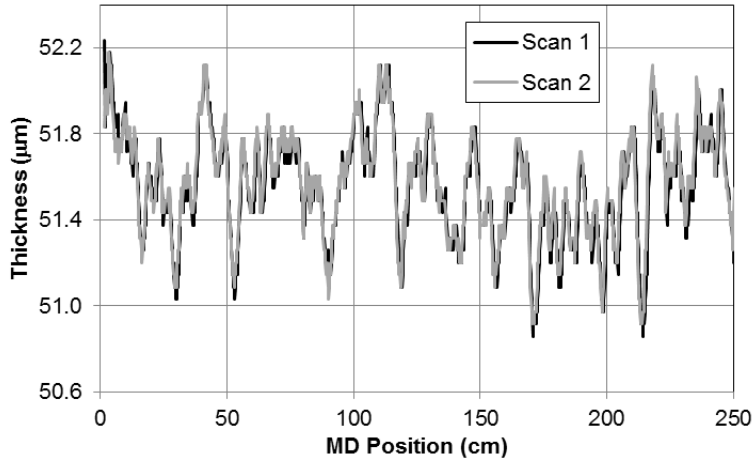

Figure 3 – Thickness of a 50 µm PET web using the SolveTech Profiler.

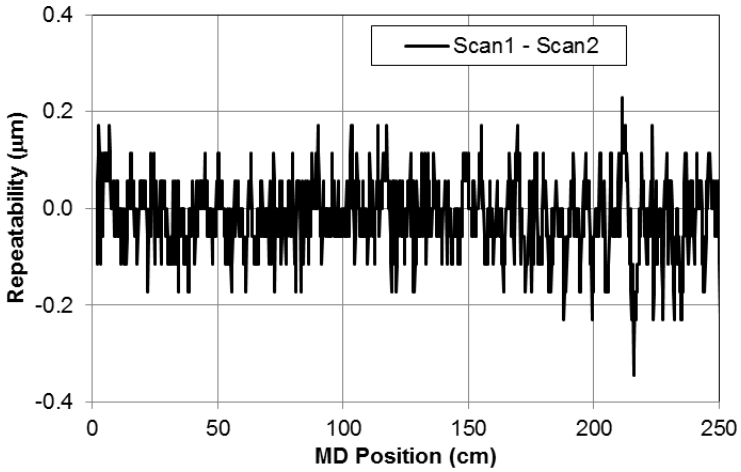

Figure 4 – Difference of Scans 1 and 2 in Fig. 3.

Both the Mesys and the SolveTech instruments were used to measure the thickness of the same strip of web 250 cm of PET film, nominally 50 µm in thickness. Again the Mesys assessed the thickness over a window 5 mm wide while the SolveTech assessed the thickness over a window 57.2 mm wide. The comparison is shown in Figure 5. The two traces are remarkably similar given that the measurement window widths and measurement methods are so different. When reviewing the sharp peaks in the traces shown in Figures 1 and 3 there could be curiosity whether the web thickness could change that rapidly in the MD or whether these peaks could be artifacts of the measurement methods. In fact these thickness variations are proven to exist herein by the repeatability demonstrated in Figures 2 and 4 and by the similarity of the traces in Figure 5.

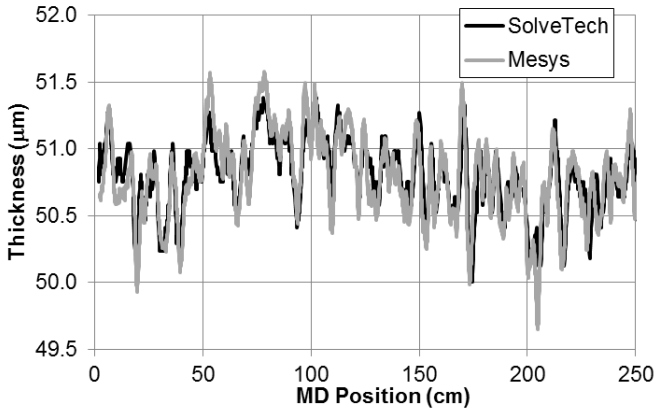

Figure 5 – Thickness Measurements for a PET web strip nominally 50 µm thick using ultrasonic and capacitance measurement methods.

FULL THICKNESS MAPPING OF AN ENTIRE WEB

With confidence that the capacitance or the ultrasonic sensing methods yielded similar results, the full mapping of the thickness of a web of larger dimensions was undertaken using the Mesys USM-200 sensor.

A PET film with a nominal thickness of 76.2 μm (0.003 in) and a 60.96 cm (24 in) width was used in this study. The map of thickness appears continuous in Fig. 6 but is not. The thickness data was acquired by parking the USM-200 sensor in a CMD location. The web was then drawn through the sensor at constant velocity and tension. Thickness data was recorded in 1.91 cm (¾ in) intervals for the entire web length of 1.2 km (3937 ft). The velocity of the web line was reversed and the web was rewound in advance of the next set of thickness measurements. The sensor was then moved 2.54 cm (1 in) in the CMD and the data collection began anew. The measurement process was conducted 24 times at the center of the 2.54 cm sectors until the discrete mapping of the entire web width had been completed.

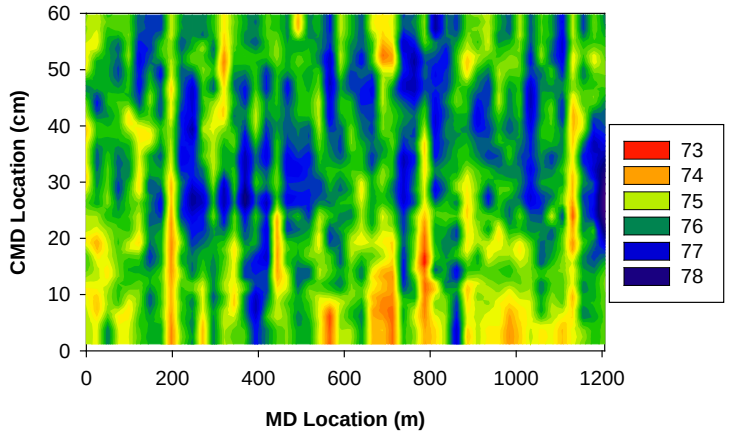

Figure 6 –Full Thickness Map of a PET web, nominally 76 μm in thickness.

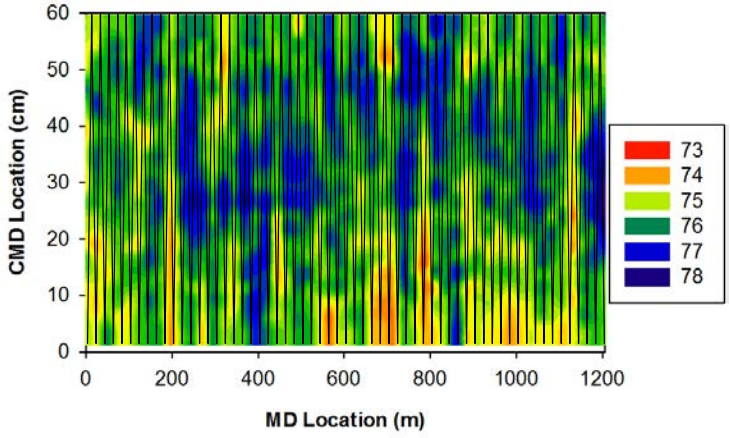

Figure 7 – Zig-Zag Traces where data from Fig. 6 was harvested.

The data in Fig. 6 will present different concerns based upon who is reviewing the data. The peak deviations from 76 μm may provide concern for those involved with downstream process requirements or from those with knowledge of the needs of the final product. The thickness variation in the MD and CMD would concern those who must wind the webs if there was understanding of how the thickness variation coupled to internal roll stresses and defects. Data for the complete thickness mapping of a web as shown in Fig. 6 are scarce. Using this data provides an opportunity to understand how the thickness traces acquired during zig-zag scans which are common in web making and coating processes relate to the total thickness variation of the web. The 60 cm wide polyester shown in Fig. 6 was slit (or cut) from an oriented parent web 349 cm wide. When manufactured the parent web was scanned with a thickness sensor 60 times.

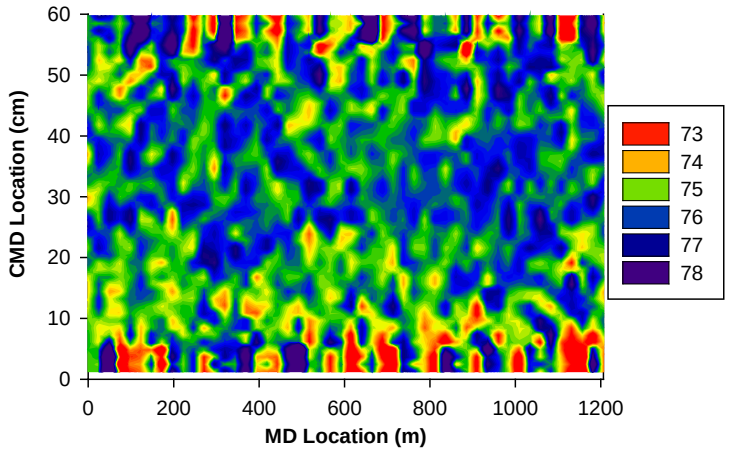

Figure 8 – Web Thickness Variation (μm) from 60 Zig-Zag Scans.

How would the web thickness presented in Fig. 6 have appeared had the data been collected in 60 zig-zag scans over the 60 cm web width? A scan consists of a zig (0 to 60 cm CMD Location) and a zag (60 to 0 cm CMD Location). In Fig. 7 the path of the thickness sensor is shown. Much less thickness data would be acquired. At the web edges data would be collected at 20 m (1200/60) intervals in comparison to the 1.91 cm data collection interval used in acquiring the data shown in Fig. 6. The data harvest was accomplished by interpolating the data from Fig. 6 at the MD locations of the 60 zig-zag scans. The web thickness in a CMD location is assumed to vary linearly from one MD location to the next where a measurement is made. In true zig-zag measurement there is no knowledge of how thickness varies at a given CMD location between the zig and the zag measurement. The new thickness data is presented in a contour plot in Fig.8. Comparing Figs. 6 and 8 it is apparent that many of the thickness features that were apparent in Fig. 6 are no longer apparent in Fig. 8. Note in Fig. 6 that many of the high and low thickness features persist in the CMD, some all the way across the web width. That persistence has been largely lost in Fig. 8. The range of thickness data is very similar per the chart legends and the overall statistics are quite comparable. For the 1,424,352 samples of data that comprise Fig. 6, the mean and standard deviation are 75.57 μm and 0.83 μm, respectively. For the 2880 samples of data that comprise Fig. 8, the mean and standard deviation are 75.63 μm and 0.81 μm, respectively.

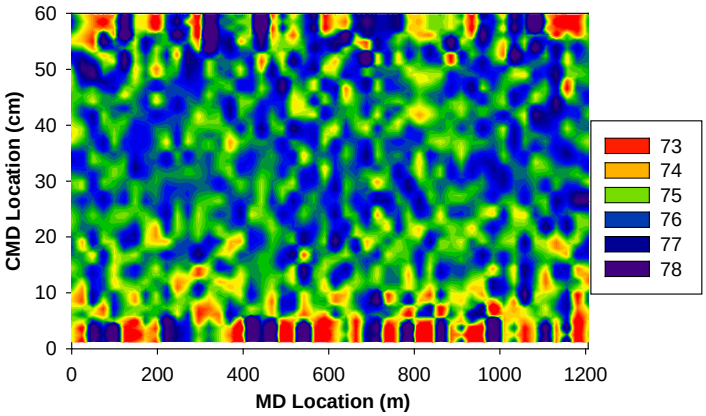

Figure 9 – Web Thickness Variation (μm) from 30 Zig-Zag Scans.

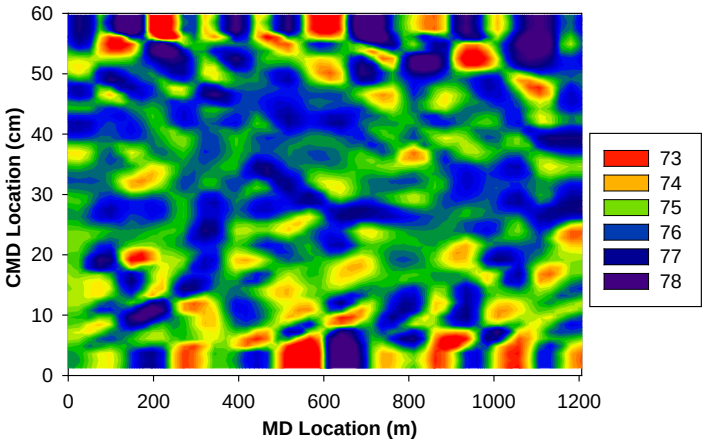

Figure 10 – Web Thickness Variation (μm) from 10 Zig-Zag Scans.

The rate of scanning is user selectable within limits for spot thickness measurement. With the method described previously the effect of scanning at other rates can be explored. In Figs. 9 and 10 thickness results are shown for 30 and 10 zig-zag scans are shown for the same web, respectively. Although there is some similarity between Figs. 8 and 9 note that shapes of local thickness features can be very different.

After the number of scans is reduced to 10 the periodicity of thickness events decreases markedly as shown in Fig. 10. The statistics of the mean and standard deviation of the thickness change little in comparison as shown in Table 1.

	Full Data Set	60 scans	30 scans	10 scans
Data Samples	1424352	2880	1440	480
Average (μm)	75.575	75.631	75.626	75.645
Standard Deviation (μm)	0.830	0.807	0.807	0.803

Table 1 – Impact of Scan Method and Sampling on Thickness Statistics.

DEVELOPING INPUT FOR AN AXISYMMETRIC WINDING MODEL

Wound roll models estimate internal stresses due to winding. The first of these models were one-dimensional and allowed the user to explore radial and tangential stresses as a function of wound roll radius [1,2]. Later models were two-dimensional and could be used to explore radial, tangential, axial and shear stresses in a plane formed by the radial and axial axes of the wound roll [3-8]. These were the first models that could be used to explore the effects of web thickness variation in the MD and CMD directions. These model developments were axisymmetric and thickness variation in the MD can vary no more rapidly than one wound roll layer. Also these models require the user to partition the web into a number of CMD sectors, 24 sectors will be chosen herein, equivalent to the number of sectors in which thickness was measured.

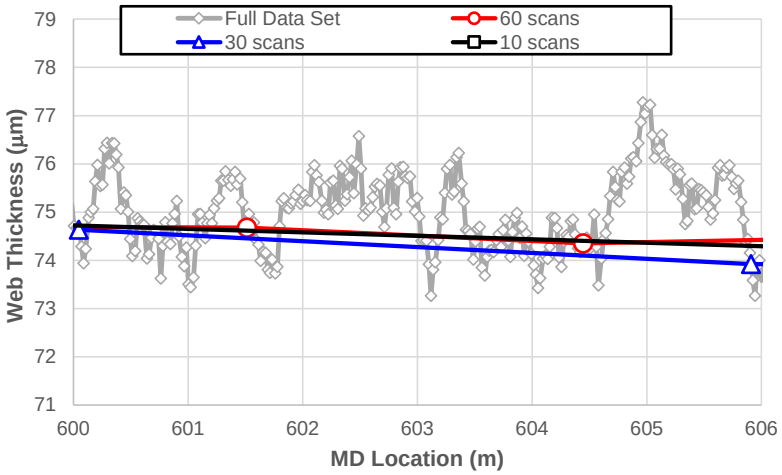

Figure 11 – Web Thickness Variation at the Lap Level in Sector 4.

The axisymmetric winding models are finite element derivations which allow linear thickness variation in the axial or CMD over the width of an element. The thickness data presented in Figs. 6, 8, 9 and 10 had to be prepared in the form of an average lap thickness for every lap in each of the 24 CMD sector locations. Each lap in every sector could have a unique average lap thickness. To illustrate this process the full thickness data along with thickness estimations from the zig-zag scans are shown for a short MD domain range in Fig. 11 for Sector 4. After 600 meters of web were wound onto the core (outer core radius of 10.16 cm), one layer in the wound roll is roughly 1 meter in length. In the full data set from Fig. 6 approximately 49 web thickness data samples were collected for each layer. Note that for all the cases of zig-zag scans that less than 1 thickness data point is being collected per layer. For the MD range shown in Fig. 11 note that no data points were collected for the 10 scans case. Linear extrapolation was employed between the measured thickness data to estimate the thickness variation in a given sector. Those estimates can differ significantly from the averages of the Full Data set over the range of one layer.

An alternative input which will be explored would be to average all data collected in a given CMD location and assume that average thickness persists in the MD.

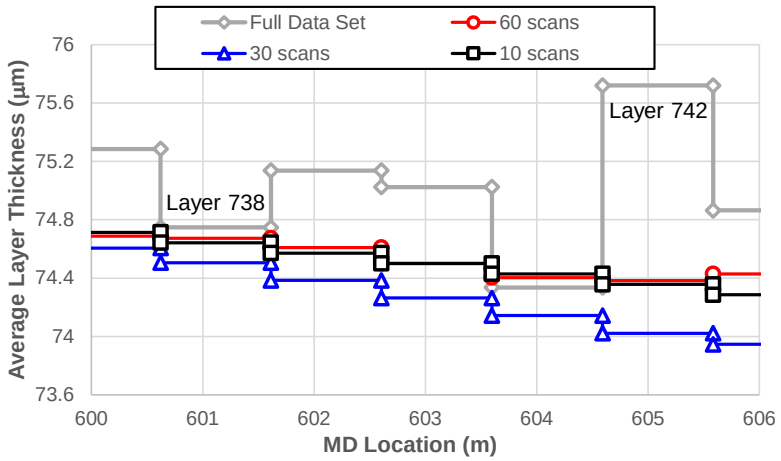

Figure 12 – Average layer Thickness in Sector 4 from Fig. 11.

Core inner radius	Core outer radius	Roll outer radius	Roll width
9.525 cm	10.16 cm	20.32 cm	60.96 cm
Core Material	Modulus	Winding Tension	Tw=3.445 MPa
E_{cr}=68.9 GPa	E_{ct}=68.9 GPa	E_{cz}=68.9 GPa	
Core Material	Poisson's Ratio		
ν_{crz}=0.33	ν_{crt}=0.33	ν_{ctz}=0.33	
Web Material	Modulus	$E_r=K_2(P+K_1)$	
E_{wt}=68.9 GPa	E_{wz}=68.9 GPa	K_1=0.01 KPa	K_2=290
Web Material	Poisson's Ratio		
ν_{wrz}=0.01	ν_{wrt}=0.01	ν_{wtz}=0.3	

Table 2 – Winding Model Input Data.

In addition to thickness variation, winding models require other geometric data, web and core material data as shown in Table 2. This data is sufficient to complete the input required for an axisymmetric winding model. The winding code employed in this research is known as MAXIWINDER and was developed at the Web Handling Research Center [7]. This code also has the ability to simulate winding with a nip roll and thermo-viscoelastic material behavior for non-uniform webs.

EXPERIMENTAL PROCEDURE

The web whose thickness variation was presented in Fig. 6 will be center wound in the laboratory at winding tension of 3.445 MPa. The web will be wound on an instrumented core developed at the Web Handling Research Center. This device is shown in Fig. 13. The core has an outer radius of 10.16 cm and is composed of 24 2.54 cm wide rings each instrumented with strain gages as shown. The web end at 1200 meters in Fig. 6 will be spliced to the core and winding will continue until the entire 1200 meters of web are wound into the roll.

Figure 13 – A Core Instrument for Measuring Core Pressure. Top: Assembled Core, Bottom Left: Switchable Output, Bottom Center: Instrumented Rings and Bottom Right: Bridge Balance.

The core was designed to be used with the winder stalled. A calibration chamber was designed to exert a hydrostatic pressure on the core. Each ring constituted one Wheatstone bridge. Each bridge had a precision adjustable resistor to null the output at zero applied pressure. Bridge power was supplied by a Micro Measurements[3] Model 3800 Wide Range Strain Indicator. The output was read on the same device.

An instrument was developed to acquire the outer layer radius as a function of CMD location, refer to Fig. 14. This instrument is a DCDT[4] (Direct Current Differential Transformer Omega Model LD500-5) follower mounted on a linear slide that could be clamped and nulled at a given wound roll radius. The follower was pushed by hand across the width of the outer layer, the CMD position was monitored by a potentiometer displacement transducer[5] (Celesco PT101-0060). The ability for a winding model to produce the current outer lap radius as a function of CMD location is important because the winding tension in the outer lap is portioned according to the outer lap radius. CMD positions where the outer lap radius is larger compared to other locations will receive a greater portion of the total winding tension. This has a significant effect on the distribution of residual stress in the wound roll [7,8].

$$T_w \sum_{j=1}^{m} A_j = \sum_{j=1}^{m} E_{\theta j} \int_0^w \int_{f_1^j(z)}^{f_2^j(z)} \frac{r - r_r}{r_r} dr dz \qquad \{1\}$$

[3] Vishay Precision Group, P.O.Box 27777, Raleigh, NC, 27611, USA.
[4] Omega Engineering, One Omega Drive, P.O. Box 4047, Stamford, CT, 06907, USA.
[5] Celesco, 20630 Plummer Street, Chatsworth, CA, 91311, USA

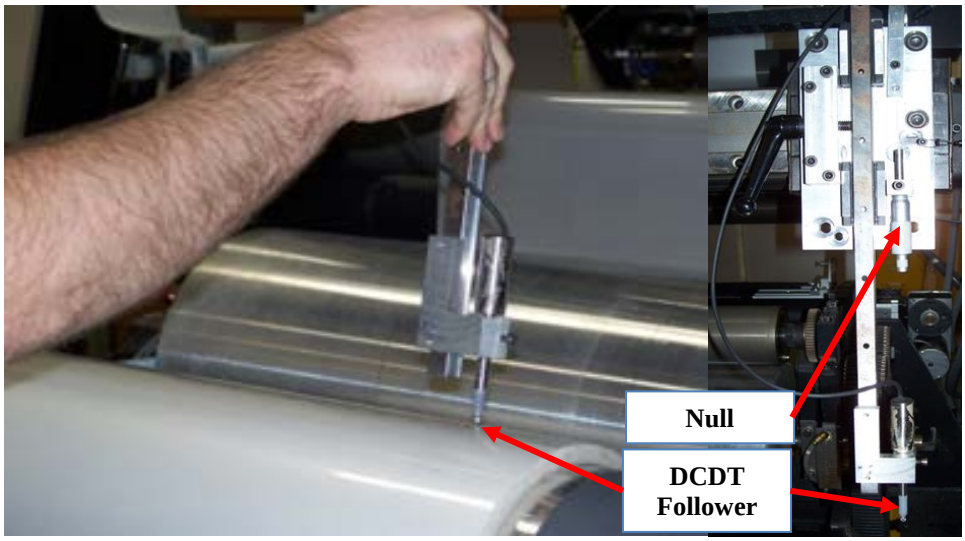

Figure 14 – Outer Layer Profilometer.

This is an equilibrium expression. The left hand side of the equation is the total winding tension in the winder tension zone, the product of the winding stress T_w and the cross sectional areas of the sectors (A_j). The right hand side involves the axisymmetric tangential stresses that are affected by the MD modulus ($E_{\theta j}$) and the tangential strains $(r-r_r)/r_r$. When integrated over the areas of all sectors a total tangent force is computed which must balance the left hand side of expression (1). In the tangent strain (r_r) is the relaxation radius which is calculated for the entire roll as a layer is added. The radius of the outer lap of a given sector is r which can vary within the domain of the element as the web thickness is allowed to vary linearly across the sector width in the axial (z) dimension. Those sectors with a larger outer lap radius (r) within a given outer layer will receive a greater portion of the winding tension than those with smaller radii. This will locally result in larger tangent stresses and pressures developing in the sectors with larger outer lap radius. Thus it is important that models compute the outer lap radius accurately and is why the outer lap radius was measured in the laboratory.

Core pressure and outer lap radius measurements will be used to benchmark the results from the axisymmetric winding code as a function of the methods used to quantify web thickness.

RESULTS

The core pressures resulting from winding tests and from the axisymmetric wound roll model are shown in Fig. 15. The test results are the average from five winding experiments and the error bars are the standard deviation of the data at that CMD location. The model results from the Full Thickness Data visually appear to agree best with the test results. The model results that used web thickness inferred from zig-zag scanning did not agree as well. The agreement improved as the frequency of scanning increased. The absolute value of the difference between the model and core pressure test result for each sector was summed to produce a total absolute error for all sectors. This error is presented in Table 3. This error initially decreases 61% from 10 to 30 scans.

When increasing from 30 to 60 scans the error decreases significantly less, only 14%. Thus there is improvement offered by additional zig-zag scanning in the context of improving winding model estimations of core pressure. There are however limits to the CMD scanning speed of thickness sensors which can limit the ability to increase the number of potential scans as a function of MD web velocity.

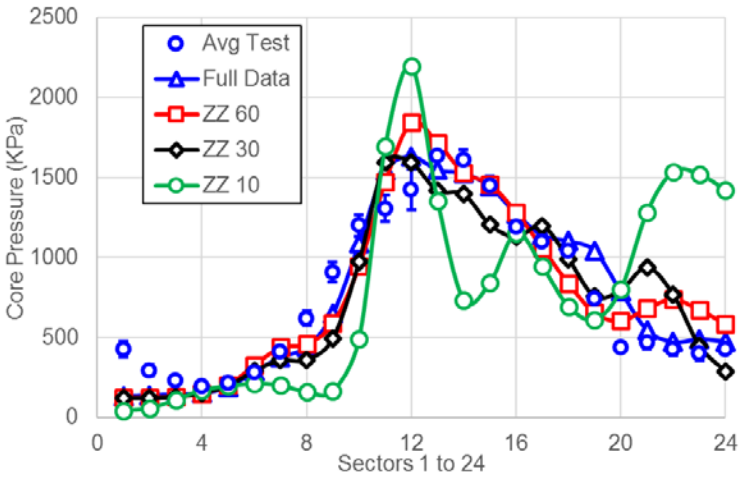

Figure 15 – Measured and Model Estimates of Core Pressure I.

The impact of averaging all thickness data in a given CMD location is seen in Fig. 16. This average thickness was calculable only because the Full Data or the zig-zag scans of thickness were already acquired. The sum error for the averaged MD thickness input is also shown in Table 3 with errors comparable to that associated with the input of a unique thickness for each layer.

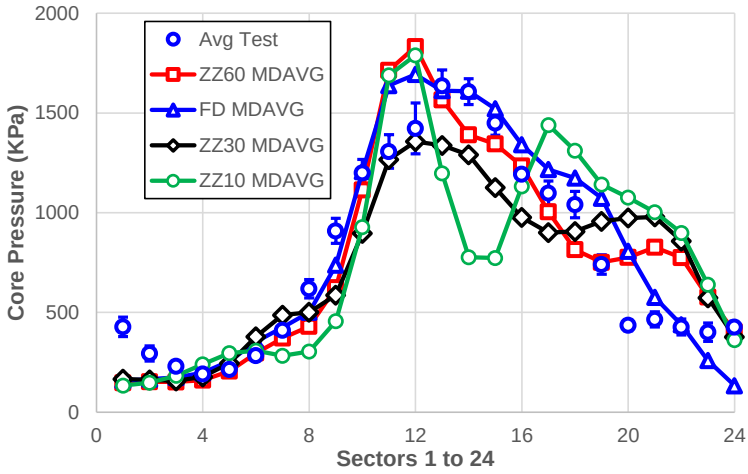

Figure 16 – Measured and Model Estimates of Core Pressure II.

Unique Layer Input Thickness	Full Data Set	60 scans	30 scans	10 scans
Sum Absolute Error (MPa)	2.91	3.72	4.33	10.97
Averaged MD Thickness	Full Data Set	60 scans	30 scans	10 scans
Sum Absolute Error (MPa)	3.98	3.24	4.94	7.53

Table 3 – Sum of Absolute Core Pressure for All Sectors.

The results showing model versus test results for the variation in the outer lap radius versus test data are shown in Fig. 17. The variation is determined by seeking the minimum value of outer lap radius and subtracting that from the radius of all sectors, for test and model results. In Fig. 17 the winding model was provided with unique thickness data for each layer and CMD location. In Fig. 18 an averaged web thickness was input for each sector. Here it is less clear visually which computed result compares best with the test results. The average test data were obtained by averaging all radius data collected within a given sector for four tests. The error bars are the standard deviation of this data. To quantify the benefit of increased scanning a total summed error term was determined and is presented in Table 4. The error was the absolute difference in outer lap radius variation between the winding model result and the average test radius in a given sector. This was summed for all sectors to provide a total error statistic. Here the Full Thickness Data was shown to model the test data most accurately. Although 30 and 60 scans provided improvement over 10 scans, note that 60 scans offered poorer agreement than the 30 scan thickness data. Although MD thickness averaging offered little benefit for the Full Data Set there was benefit for the zig-zag data.

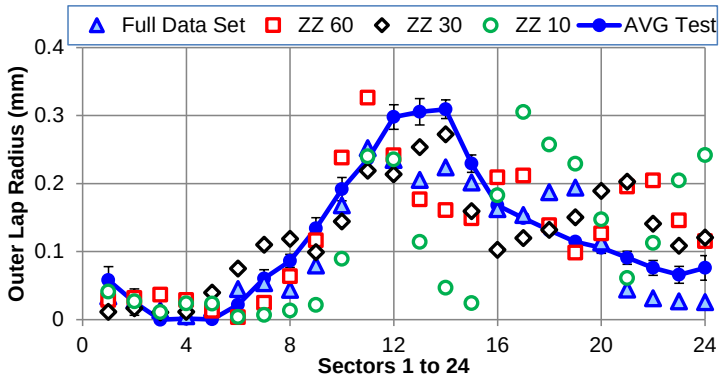

Figure 17 – Measured and Model Estimates of Outer Lap Radius I.

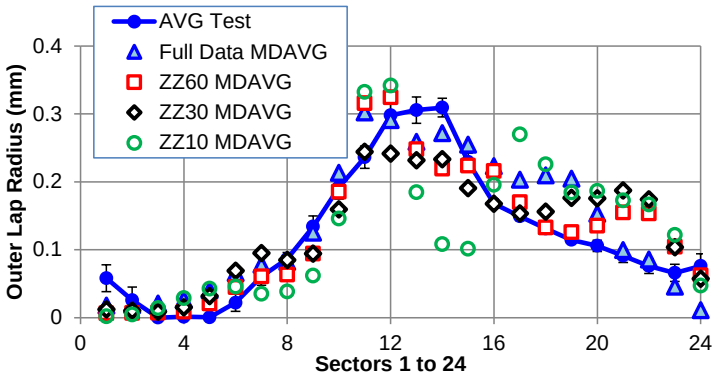

Figure 18 – Measured and Model Estimates of Lap Radius II.

Layer Input Thickness	Full Data Set	60 scans	30 scans	10 scans
Sum Absolute Error (mm)	0.837	1.257	1.067	1.983
Averaged MD Thickness	Full Data Set	60 scans	30 scans	10 scans
Sum Absolute Error (mm)	0.839	0.762	0.934	1.616

Table 4 – Sum of Absolute Outer Lap Radius Error for All Sectors.

The experimental measurements used are boundary values. The stresses output by the winding model can also be studied spatially between the core and the outer layer. Sector 14 had the highest core pressure measurement for any sector. The pressure as a function of wound roll radius is shown in Fig. 19. If the Full Thickness Data is input to the winding model the results show the pressure varies from a value close to the measured core pressure at the outer core radius to zero at the outer wound roll radius. Note that increased number of zig-zag scans agree better with the results from the Full Thickness Data set. Similar to the core pressure results shown in Fig. 15 much improvement occurs between 10 and 30 scans and less improvement when moving from 30 to 60 scans.

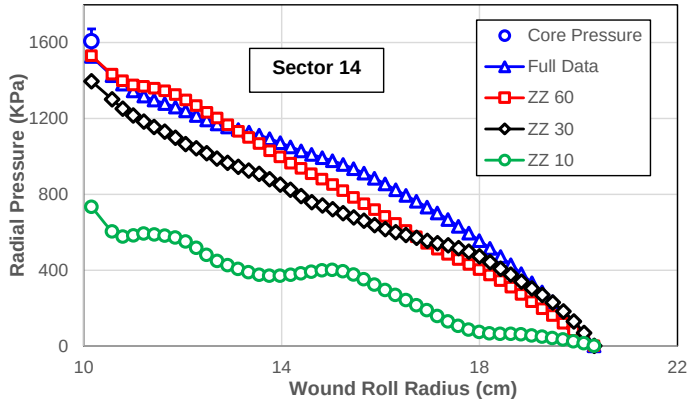

Figure 19 – Radial Pressure in Sector 14.

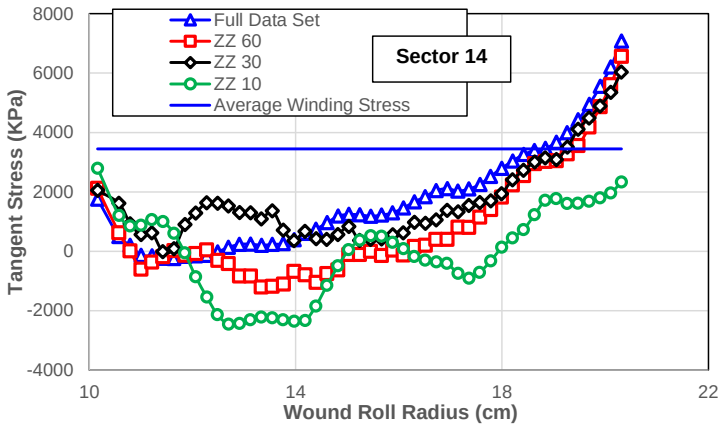

Figure 20 – Tangent Stress in Sector 14.

The tangential stresses for sector 14 are shown in Fig. 18. From 10 to 19 cm of wound roll radius the 60 scan case shows the best agreement with the Full Thickness Data set. From 19 cm to the outer radius of the roll the 30 scan case agrees best. Beyond that there is similarity with other charts showing considerable improvement between 10 and 30 scans but less improvement when increasing from 30 to 60 scans.

The pressures and stresses in Figs. 19 and 20 are smoothed considerably if average web thickness is input to the winding model as shown in Figs. 21 and 22. The benefit of increased scanning is witnessed again. The Full Data set produced average thicknesses that when input to the winding model provided good agreement with measured core pressure in Fig. 21. It appears that thickness data averaged in the MD is a good input for a winding model provided that the average results from sufficient scans.

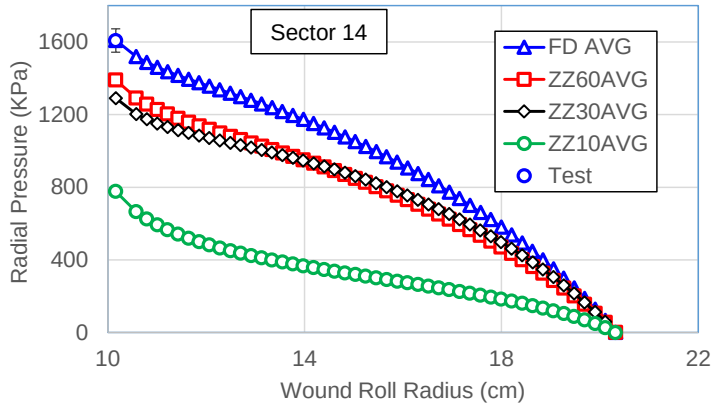

Figure 21 – Radial Pressure in Sector 14.

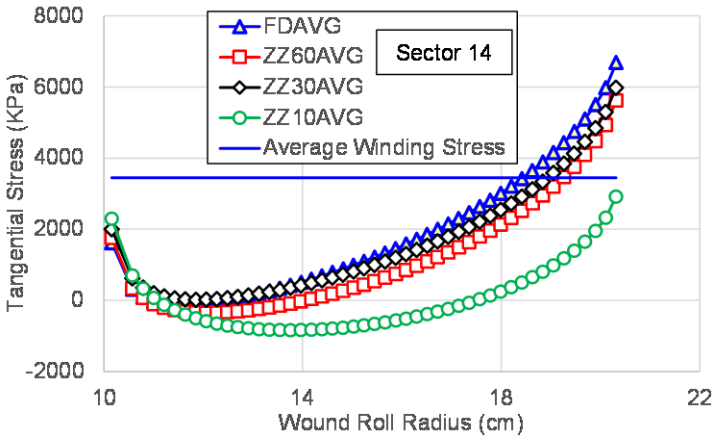

Figure 22 – Tangent Stress in Sector 14.

The winding models allow the study of error spatially. The pressures, tangential stresses, axial and shear stresses output from the model for the Full Thickness Data set are presented in Figs. 23 through 26, respectively. To study the spatial error the absolute difference in pressure between each the pressure data presented in Fig. 23 was formed for the 10, 30 and 60 zig-zag scan cases and then summed. The spatial error for the tangential stresses was formed similarly. These errors are presented in Table 5. The winding code parses the output to provide 48 data points in the radial direction for each of the 24 sectors for this model. Thus the error sums are for 1152 data points and summed error is also shown after averaging.

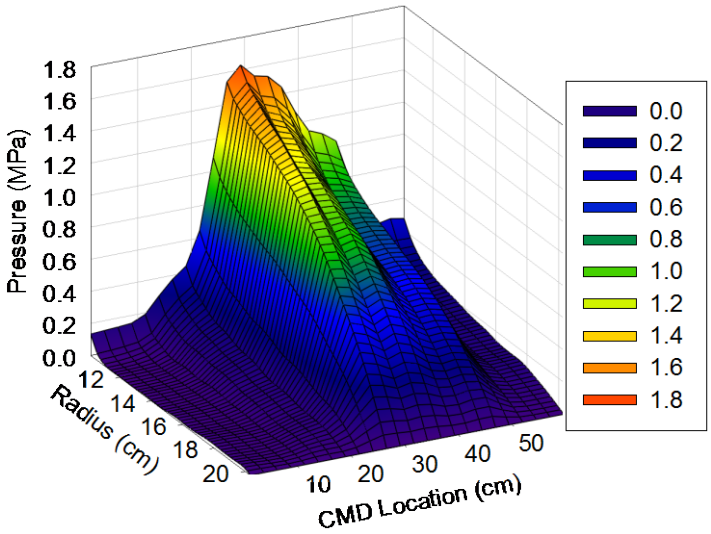

Figure 23 – Pressure in Wound Roll.

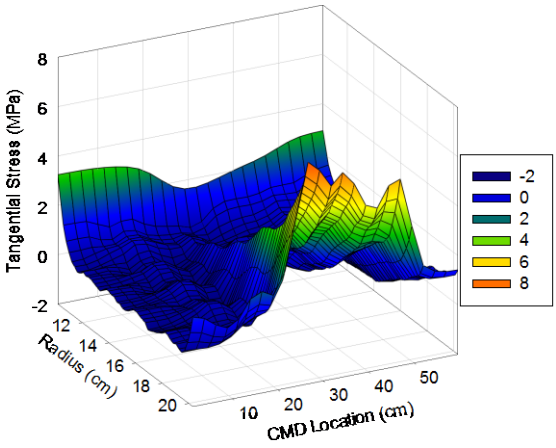

Figure 24 – Tangent Stress in Wound Roll.

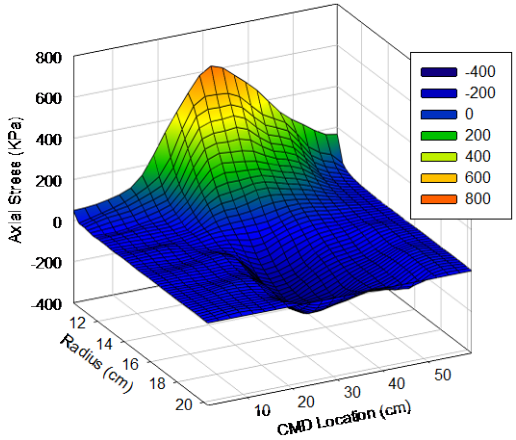

Figure 25 – Axial Stress in Wound Roll.

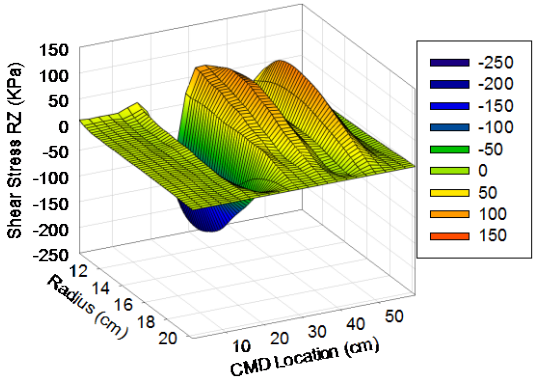

Figure 26 – Shear Stress in Wound Roll

Sum Spatial Error	60 scans	30 scans	10 scans
Pressure (MPa)	92.5	134.8	226.2
Pressure (MPa)/1152	0.080	0.117	0.196
Tangential Stress (MPa)	503.2	693.4	973.7
Tangential Stress (MPa)/1152	0.437	0.602	0.845

Table 5 – Sum of Spatial Errors for Pressure and Tangential Stresses.

The errors in Table 5 are based entirely on the winding model results. The benefit of increased scanning is very apparent. The spatial error is also a good method for determining the effect of the input of an averaged MD web thickness for each sector rather than the unique layer input and is shown in Table 6.

Sum Spatial Error	Full Data AVG	60ZZ AVG	30ZZ AVG	10ZZ AVG
Pressure (MPa)	45.9	99.0	127.0	189.3
Pressure (MPa)/1152	0.040	0.086	0.110	0.164
Tangential Stress (MPa)	235.0	409.8	411.7	680.3
Tangential Stress (MPa)/1152	0.204	0.356	0.357	0.591

Table 6 – Spatial Errors for Pressure and Tangential Stresses for MD Average Web Thickness Input.

When comparing Tables 5 and 6, there appears to be a significant benefit for this web to input an average MD thickness per sector if zig-zag scanning has been employed. The effect is more significant for the tangential stresses than the pressures. When zig-zag scanning, it is possible to measure values of web thickness that could be extreme values near the minimum or maximum web thickness. If so the extreme value of thickness could affect the interpolated thickness values for many layers, dependent on the number of zig-zag scans, refer to Figs. 11 and 12. By using the average all of the web thickness measurements made at a given CMD location during zig and zag scans, the impact of extreme thickness measurements producing extreme wound roll stresses is decreased.

CONCLUSIONS

The following conclusions were drawn as a result of this study:

- The transmitting ultrasonic method of thickness measurement was found to yield thickness measurements essentially equal to those measured using the capacitance method for inferring the thickness of a polyester web.
- Measurement of the web thickness in all sectors provided better definition of web thickness variation than can be obtained with zig-zag scanning. Comparison of Figs. 6 and 8 shows that thickness variations that persist in the CMD are not visible when zig-zag scanning is used.
- There was no benefit of increased zig-zag scanning on the overall thickness mean and standard deviation shown in Table 1.

- Based on comparison to both core pressure and outer lap radius variation measurement the zig-zag scanning provides an inferior thickness input in comparison to a full thickness map for winding models.
- The benefit of increased zig-zag scanning in providing improved resolution in pressure and stresses were shown in Figs. 17 and 18 and in Table 5.
- There was benefit to averaging all the web thickness data at a given CMD location for input to the winding model when zig-zag scanning thickness measurement is employed. Trends remained similar as increased scanning provided better estimates of the average web thickness, refer to the results in Tables 3, 4, 5 and 6.

REFERENCES

1. Hakiel, Z., "Nonlinear Model for Wound Roll Stresses," TAPPI Journal, Vol. 70, No. 5, May 1987, pp. 113-117.
2. Willett, M.S. and Poesch, W.L., "Determining the Stress Distributions in Wound Reels of Magnetic Tape Using Nonlinear Finite Difference Approach," Journal of Applied Mechanics, Vol. 5, June 1988, pp. 365-371.
3. Cole, Kevin A. and Hakiel, Z., "Nonlinear Wound Roll Stress Model accounting for widthwise Web Thickness non-uniformities," ASME, AMD, Vol. 149, 1992, pp. 12-24.
4. Kedl, Douglas M., "Using a Two Dimensional Winding Model to Predict Wound Roll Stresses that Occur Due to Circumferential Steps in Core Diameter or to Cross-Web Caliper Variation," Proceedings of the Second International Conference on Web Handling. Oklahoma State University, May 19-22, 1992, pp. 99-112.
5. Lee, Y. M. and Wickert, J. A., "Stress Field in Finite Width Axisymmetric Wound Rolls," ASME Journal of Applied Mechanics, Vol. 69, No. 2, 2002, pp. 130-138.
6. Hoffecker, P. and Good, J. K. "Tension Allocation in Three Dimensional Wound Roll," Proceedings of the Eighth International Conference on Web Handling. Oklahoma State University, Stillwater, Oklahoma, June 5-8, 2005, pp. 565-581.
7. Mollamahmutoglu, C. and Good, J.K. "Axisymmetric Wound Roll Models," Proceedings of the Tenth International Conference on Web Handling. Oklahoma State University, Stillwater, Oklahoma, June 7-10, 2009, pp. 105-130.
8. Mollamahmutoglu, C. and Good, "Modeling the Influence of Web Thickness and length Imperfections Resulting from Manufacturing Processes on Wound Roll Stresses," CIRP Journal of Manufacturing Science and Technology, V8, January 2015, pp. 22-33.